Cell Reports
Article

A Proteomic Characterization of Factors Enriched at Nascent DNA Molecules

Andres J. Lopez-Contreras,[1,7] Isabel Ruppen,[2,7] Maria Nieto-Soler,[1] Matilde Murga,[1] Sara Rodriguez-Acebes,[3] Silvia Remeseiro,[4] Sara Rodrigo-Perez,[1] Ana M. Rojas,[5,6] Juan Mendez,[3] Javier Muñoz,[2] and Oscar Fernandez-Capetillo[1,*]
[1]Genomic Instability Group
[2]Proteomics Unit
[3]DNA Replication Group
[4]Chromosome Dynamics Group
Spanish National Cancer Research Centre (CNIO), Madrid 28029, Spain
[5]Computational Cell Biology Group, Institute for Predictive and Personalized Medicine of Cancer, Badalona 08916, Spain
[6]Life Sciences Department, Barcelona Supercomputing Center, Barcelona 08034, Spain
[7]These authors contributed equally to this work and are co-first authors
*Correspondence: ofernandez@cnio.es
http://dx.doi.org/10.1016/j.celrep.2013.03.009

SUMMARY

DNA replication is facilitated by multiple factors that concentrate in the vicinity of replication forks. Here, we developed an approach that combines the isolation of proteins on nascent DNA chains with mass spectrometry (iPOND-MS), allowing a comprehensive proteomic characterization of the human replisome and replisome-associated factors. In addition to known replisome components, we provide a broad list of proteins that reside in the vicinity of the replisome, some of which were not previously associated with replication. For instance, our data support a link between DNA replication and the Williams-Beuren syndrome and identify ZNF24 as a replication factor. In addition, we reveal that SUMOylation is widespread for factors that concentrate near replisomes, which contrasts with lower UQylation levels at these sites. This resource provides a panoramic view of the proteins that concentrate in the surroundings of the replisome, which should facilitate future investigations on DNA replication and genome maintenance.

INTRODUCTION

Faithful duplication of the genome is essential in limiting mutations and preserving genome integrity. In addition to base changes, difficulties in the progression of the replication fork lead to the accumulation of recombinogenic stretches of single-stranded DNA (ssDNA), which leads to deletions, duplications, or complex genome rearrangements. This pathological accumulation of ssDNA at replication forks is known as replicative stress (RS) and has been associated to cancer and aging (Cimprich and Cortez, 2008; López-Contreras and Fernandez-Capetillo, 2010). Besides DNA polymerases, DNA replication demands the activity of numerous proteins (reviewed in Hübscher, 2009). For instance, the processing of Okazaki fragments alone requires at least 23 polypeptides (Maga et al., 2001). In addition to those factors directly involved in DNA replication, proteins involved in DNA repair, cell-cycle checkpoints, or chromatin remodeling are also enriched in the proximity of the replisomes. This is best exemplified by the concept of "replication factories" (Cook, 1999), where several replisomes and accessory factors are concentrated in a small nuclear volume, thereby facilitating an appropriate supply of all the activities needed to ensue genome duplication.

Replication factories are easily detected as discrete nuclear foci of the proliferating cell nuclear antigen (PCNA), and their size and location accurately indicate replication timing, numerous small euchromatic foci in early S phase, perinuclear and perinucleolar foci in mid S phase, and a reduced number of large heterochromatic foci in late S phase (Leonhardt et al., 2000). This property has been previously used to illustrate the presence of nonreplisome proteins at replication factories such as the DNA repair protein MRE11 (Mirzoeva and Petrini, 2003) or the DNA methyltransferase DNMT1 (Estève et al., 2006). However, immunofluorescence faces important limitations such as the need for suitable and specific antibodies, its limited throughput, and, most importantly, the levels of a protein that are needed for its detection. For instance, key components of the replisome, such as the MCM helicase, cannot be detected at replication factories by immunofluorescence (reviewed by Laskey and Madine, 2003). This has recently been shown to be due to the low protein abundance and partial chromatin decondensation coupled to DNA synthesis (Aparicio et al., 2012). In order to overcome these limitations, several approaches have been attempted. Successful studies in yeast have used immunoprecipitation of tagged replisome components followed by mass spectrometry (MS) (Gambus et al., 2006; 2009). This approach, however, only detects proteins that are directly or indirectly associated to replication factors, and, therefore, misses additional factors that might be concentrated in the vicinity of replication forks.

Immunoprecipitation of newly replicated DNA offers an attractive alternative to the methodologies mentioned above. For instance, immunoprecipitation of 5′-Bromo-2′-deoxyuridine

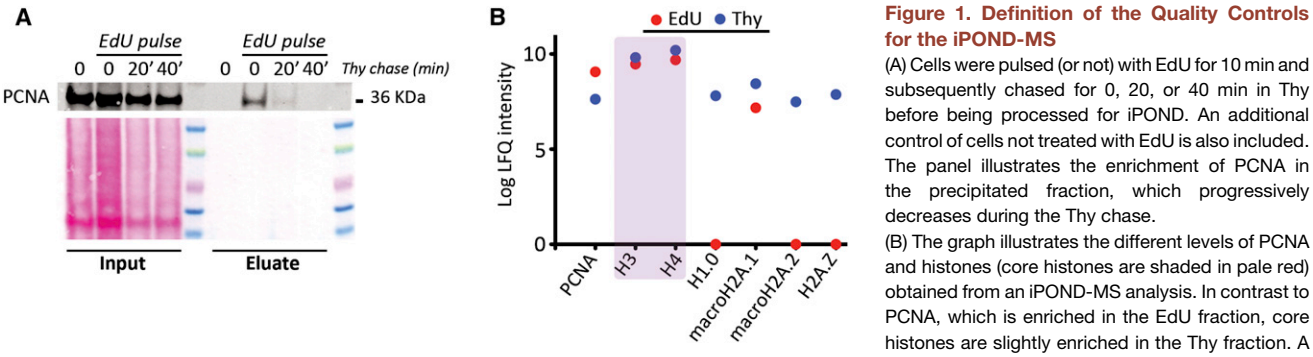

Figure 1. Definition of the Quality Controls for the iPOND-MS

(A) Cells were pulsed (or not) with EdU for 10 min and subsequently chased for 0, 20, or 40 min in Thy before being processed for iPOND. An additional control of cells not treated with EdU is also included. The panel illustrates the enrichment of PCNA in the precipitated fraction, which progressively decreases during the Thy chase.

(B) The graph illustrates the different levels of PCNA and histones (core histones are shaded in pale red) obtained from an iPOND-MS analysis. In contrast to PCNA, which is enriched in the EdU fraction, core histones are slightly enriched in the Thy fraction. A further enrichment of the linker histone H1 and H2A variants is also seen in the Thy fraction.

was used to evaluate the dynamics of RAD51 at stalled or broken replication forks (Petermann et al., 2010). However, the detection of halogenated nucleoside derivatives involves the use of aggressive experimental conditions which are needed to denature DNA and significantly damage proteins. A major technical improvement came from the incorporation of Click chemistry to nucleoside derivatives (Kolb et al., 2001). During DNA replication, 5′-ethynyl-2′-deoxyuridine (EdU) can be taken up by live cells and incorporated into DNA. Subsequently, Click chemistry can covalently conjugate molecules to EdU under mild conditions that do not demand DNA denaturation. For example, the conjugation of fluorochromes to EdU has facilitated the microscopy- or cytometry-mediated analysis of DNA replication (Cappella et al., 2008; Salic and Mitchison, 2008).

In 2011, two independent groups used EdU conjugated to biotin through Click chemistry to immunoprecipitate nascent DNA molecules and their associated proteins. These two protocols, named isolation of proteins on nascent DNA (iPOND) and DNA-mediated chromatin pull-down (Dm-ChP), respectively (Kliszczak et al., 2011; Sirbu et al., 2011), use highly specific streptavidin-biotin binding to pull down nascent DNA molecules from cells exposed to short pulses of EdU. Previous crosslinking with formaldehyde allows both procedures to pull down factors that are associated with recently replicated DNA. In the case of Dm-ChP, a proteomic analysis was made on the proteins that are pulled down through EdU-chromatin pull-down (Kliszczak et al., 2011). However, the experiment compared proteins that were pulled down with streptavidin from cells treated with EdU with those pulled down from cells that were not exposed to EdU. Therefore, this work mostly found proteins that were bound to DNA or chromatin but not necessarily enriched at replication forks. An interesting technical variation to this part was implemented on the iPOND pipeline (Sirbu et al., 2011; 2012), in which the EdU pulse was followed via a thymidine chase. This second period is important, given that it displaces the EdU-positive DNA away from the replication fork. In this case, it is possible to discriminate proteins that are enriched on nascent DNA molecules from those that are generally found associated to DNA. However, no proteomic characterization with iPOND has been reported so far. Here, we used iPOND followed by MS (iPOND-MS) to identify proteins that are enriched on the vicinity of the replisome. By incorporating the thymidine chase to the pipeline, increasing the number of cells to facilitate the detection of low-abundance proteins, fine-tuning of the chromatin isolation protocol, and analyzing a high number of biological replicates, we have been able to obtain a robust data set of proteins enriched at nascent DNA molecules. We are confident that this resource constitutes the most comprehensive characterization of the human replisome and replisome-associated factors available to date.

RESULTS

Defining the Conditions for iPOND-Based Proteomics

To purify proteins that are enriched on nascent DNA, we used a slightly modified version of the iPOND protocol (Sirbu et al., 2012) (see Experimental Procedures). Total cell numbers per condition were increased in order to facilitate the detection of less abundant proteins. In addition, we reasoned that using smaller chromatin fragments could facilitate the purification of proteins that are closer to the replisome. Therefore, we introduced variations on the sonication protocol that allow the purification of DNA fragments of around 80 bp. This is the minimum fragment size at which the iPOND protocol could efficiently pull down chromatin.

The efficiency of iPOND was first determined by testing the enrichment of the DNA clamp PCNA in the EdU fraction (Figure 1A). A 10 min EdU pulse followed by iPOND led to the detection of PCNA on precipitated chromatin. A subsequent chase period in thymidine displaced the EdU-labeled DNA away from the replication fork. Then, we defined the chase time that was needed so that PCNA was not found on the precipitated chromatin. After a 40 min chase, no PCNA could be detected on the precipitated fraction. To ensure that the replication fork was effectively separated from the EdU-labeled DNA but also to limit the potential effects of a prolonged exposure to thymidine, we decided to use a chase time of 60 min for the subsequent experiments.

Then, we performed iPOND using 3×10^8 HEK293T cells per sample and compared (a) 10 min EdU (EdU) and (b) 10 min EdU followed by 60 min thymidine (Thy) samples by MS. Enriched proteins were determined by label-free quantification (LFQ) intensities, as calculated by MaxQuant software (Luber et al., 2010). As a quality control, we verified that PCNA was enriched in the EdU sample before analyzing the experiment by MS. After processing the sample by MS, we also looked at the levels of the

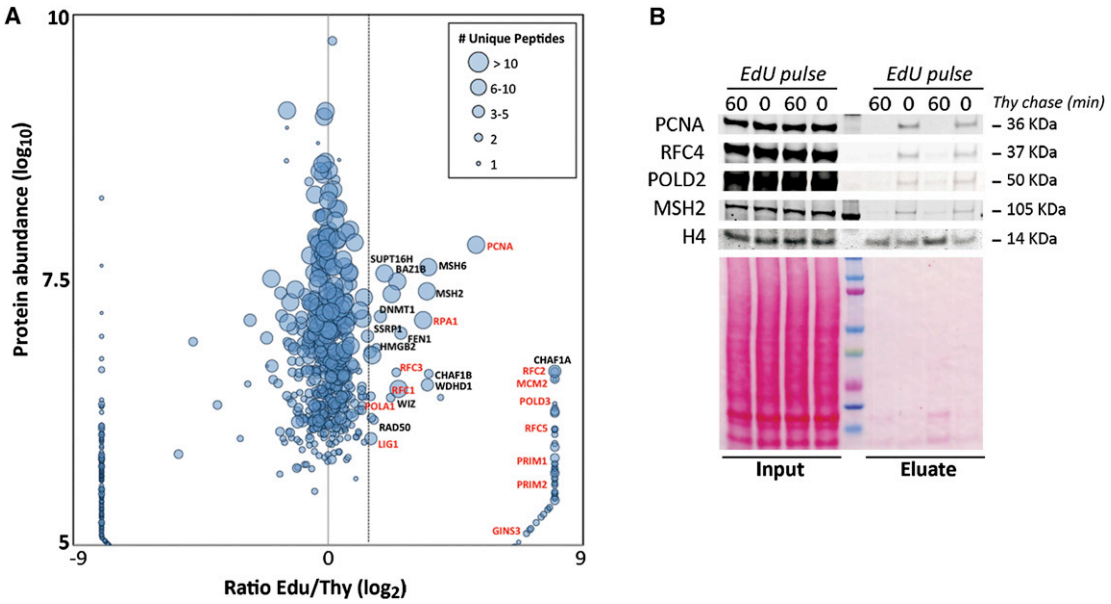

Figure 2. Identification of Proteins Enriched in Nascent DNA by iPOND-MS

(A) Protein abundances, calculated from the average of LFQ intensity (log_{10}) in EdU and Thy fractions, are plotted against the ratio of LFQ intensity (log_2) between EdU and Thy samples. The size of each spot reflects the number of unique peptides used to calculate protein ratios. The dotted line represents an EdU enrichment cutoff value of 1.5. The location of some well-established replication proteins is indicated in red, and the location of replication-associated proteins is in black. (B) Levels of PCNA, RFC4, POLD2, MSH2, and H4 from two independent experiments that were further analyzed by MS are shown. The left lanes illustrate the levels on the input samples, and the right lanes illustrate the iPOND extracts from cells exposed to a 10 min pulse of EdU, followed (or not) by a 60 min chase in Thymidine.

core histones as an additional control to ensure that chromatin was being precipitated in both fractions. In a typical experiment, levels of the core histones were slightly enriched on the Thy fraction, which could be due to the presence of ssDNA or chromatin-devoid double-stranded DNA on the EdU fraction that is closer to the replisome (Figure 1B). Histone H1 was almost exclusively detected on the Thy fraction, consistent with the delayed loading of linker histones to chromatin during replication (Worcel et al., 1978; Sirbu et al., 2011). Interestingly, the histone H2A variants macroH2A.2 and H2AZ were also highly enriched on the Thy fraction, which could reflect that the loading of these histone variants might occur independently of nucleosome reassembly during replication and be more related to the de novo establishment of facultative heterochromatin or transcriptionally inactive promoters (Costanzi and Pehrson, 1998; Mizuguchi et al., 2004; Zhang et al., 2005). Interestingly, a recent report found that a fraction of H2AZ-containing nucleosomes that are present in G1 are depleted from chromatin during S phase, which would be consistent with our observations (Nekrasov et al., 2012). For the iPOND-MS data used in this manuscript, we restricted our analyses to those experiments where PCNA showed a clear enrichment on the EdU sample and core histones were partially enriched on Thy samples.

A Proteomic View of Nascent DNA Molecules

By following the protocol and quality controls described above, we ended up with six biological replicates of iPOND-MS. Notably, a comparison of protein abundances by proteomics in any of these experiments consistently identified most of the known replisome components among the highest enriched in the EdU fraction. These included components of the DNA polymerases, primase, helicase, replication protein A (RPA), PCNA, and all five subunits of the clamp loader complex replication factor C (RFC). A representative example from an iPOND-MS is shown in Figure 2A. In addition to bona fide replisome components, all these analyses revealed the enrichment on the EdU sample of additional proteins that have directly or indirectly been related to replication, and some of which are not known to be clearly linked to replication. One of the proteins that consistently showed a very high enrichment on precipitated nascent DNA was the mismatch repair (MMR) protein MSH2. Previous work had already shown a direct interaction between PCNA and the MMR proteins MSH6 and MSH3 (Clark et al., 2000), which could target these two proteins to replication factories (Jiricny, 2006). A validation by western blot (WB) from two independent experiments is shown in Figure 2B. Altogether, the data above demonstrate that the experimental approach we used was able to identify proteins that are either directly linked to the replisome or which are abundant in the vicinity of the replisome, such as at replication factories.

To minimize the experimental noise that could derive from the iPOND-MS pipeline, we combined the data coming from all six experiments that passed the quality controls and selected those proteins that showed enrichments greater than 8-fold in at least all experiments but one in which they were detected by MS. After applying these high-stringency filters, we ended up with a list of 48 proteins that are illustrated in Table 1 (the entire data set for the six experiments is available in Table S1). The

Table1. List of Proteins Enriched on Nascent DNA Molecules by iPOND-MS

Gene Name	Alias	Enrichment (log2)	No. of Reps
Proliferating cell nuclear antigen	**PCNA**	9.25	6 (6)
DNA mismatch repair protein Msh6	**MSH6**	9.00	6 (6)
DNA mismatch repair protein Msh2	**MSH2**	8.02	6 (6)
DNA mismatch repair protein Msh3	**MSH3**	6.52	6 (6)
Replication factor C subunit 1	**RFC1**	8.86	6 (6)
Replication factor C subunit 4	**RFC4**	8.33	6 (6)
Replication factor C subunit 2	**RFC2**	7.95	6 (6)
Replication factor C subunit 3	**RFC3**	7.63	6 (6)
Replication factor C subunit 5	**RFC5**	6.85	5 (6)
Chromatin assembly factor 1 subunit A	**CHAF1A**	8.07	6 (6)
Chromatin assembly factor 1 subunit B	**CHAF1B**	8.01	6 (6)
Replication protein A 70 kDa DNA-binding subunit	**RPA1**	8.70	6 (6)
Replication protein A 32 kDa subunit	**RPA2**	6.54	6 (6)
DNA polymerase alpha catalytic subunit	**POLA1**	7.83	5 (5)
DNA polymerase delta catalytic subunit	**POLD1**	7.15	4 (5)
DNA polymerase delta subunit 3	**POLD3**	6.02	4 (5)
DNA polymerase epsilon catalytic subunit A	**POLE**	5.25	4 (5)
Chromosome transmission fidelity factor 4 homolog	**CTF4**	7.43	6 (6)
DNA ligase 1	**LIG1**	7.39	5 (5)
DNA primase large subunit	**PRIM2**	6.79	5 (5)
Exonuclease 1	**EXO1**	6.34	4 (4)
Ribonuclease H2 subunit B	**RNASEH2B**	5.07	3 (4)
Flap endonuclease 1	**FEN1**	3.71	6 (6)
DNA replication licensing factor MCM2	**MCM2**	*5.50*	*2 (3)*
DNA replication licensing factor MCM4	**MCM4**	3.85	4 (5)
DNA replication licensing factor MCM5	**MCM5**	3.34	3 (5)
DNA replication licensing factor MCM3	***MCM3***	*1.94*	*3 (5)*
DNA replication licensing factor MCM6	***MCM6***	*1.88*	*4 (6)*
DNA replication licensing factor MCM7	***MCM7***	*1.63*	*3 (5)*
DNA replication complex GINS protein PSF3	**GINS3**	4.47	4 (5)
FACT complex subunit SPT16	**SUPT16H**	3.73	6 (6)
FACT complex subunit SSRP1	**SSRP1**	3.45	6 (6)
Protein Wiz	**WIZ**	7.33	4 (5)
Histone-lysine N-methyltransferase EHMT1	**GLP**	5.93	3 (3)
DNA (cytosine-5)-methyltransferase 1	**DNMT1**	4.46	6 (6)
Histone-lysine N-methyltransferase EHMT2	**G9A**	4.44	4 (5)
E3 ubiquitin-protein ligase UHRF1	**UHRF1**	4.43	4 (5)
Double-strand break repair protein MRE11A	**MRE11A**	6.89	5 (5)
DNA repair protein RAD50	**RAD50**	5.18	4 (5)
Williams syndrome transcription factor	**WSTF**	6.27	6 (6)
Probable global transcription activator SNF2L1	**SNF2L1**	5.85	4 (5)
General transcription factor II-I	**GTF2I**	2.64	5 (6)
Sucrose nonfermenting protein 2 homolog (SNF2H)	***SNF2H***	*1.95*	*5 (6)*
Protein phosphatase 1E	**PPM1E**	8.43	3 (3)

(*Continued on next page*)

Table1. *Continued*

Gene Name	Alias	Enrichment (log2)	No. of Reps
Zinc finger protein 24	**ZNF24**	6.17	3 (3)
ATPase family AAA domain-containing protein 5	**ATAD5**	6.35	3 (3)
60S acidic ribosomal protein P1	**RPLP1**	5.83	5 (5)
Tubulin beta-4A chain	**TUBB4A;TUBB4**	5.17	4 (5)
60S ribosomal protein L11	**RPL11**	5.05	5 (6)
DnaJ homolog subfamily A member 1	**DNAJA1**	4.92	4 (5)
Ataxin-10	**ATXN10**	4.09	3 (4)
Transcription elongation factor A protein 1	**TCEA1**	4.04	3 (4)

The cutoff was set in those proteins that were enriched more than 8-fold on the EdU sample (versus Thy) in at least all the experiments in which they were detected except for one. The table also includes four proteins (MCM3, MCM6, MCM7, and SNF2H) which were also enriched in the EdU samples but are below the threshold and were included for comparison with the other members of the functional group (gray background). Numbers indicate the number of experiments in which the protein was enriched above the established cut-off. Bracketed numbers indicate the number of experiments in which the protein was detected by MS.

table was ordered by mean enrichment and structured by functional groups. Then, the groups were ordered on the basis of the highest enrichment shown by a member of the group. Ingenuity Pathway Analysis (IPA) (http://www.ingenuity.com) of functional networks with the use of this list detected "DNA Replication, Recombination and Repair" as the most significant category within the "Molecular and Cellular Functions" section ($p = 5.24 \times 10^{-17}$). Moreover, a STRING analysis of the list for known and predicted protein-protein interactions (http://string-db.org) showed a highly cohesive network and revealed abundant functional interactions within the members of most of the groups that we used in our categories (Figure 3). A brief description of the known roles of these proteins and their links to replication is provided in the Discussion.

It is worth stressing that the list of 48 proteins that passed our stringency filters is not the full list of proteins detected by MS (which is available in Table S1). In fact, other replisome or replisome-associated proteins were also enriched on nascent DNA molecules (i.e., TOP2A, TOP2B, RNASEH2A, PRIM1, SMARCAD1, POLA2, etc.), although they were frequently below the level of detection of the MS and, therefore, did not make the final cutoff. Further inspection of the full list reveals additional interesting aspects, such as an accumulation of SUMO peptides on the EdU fraction. In agreement with this, we consistently detected a ladder of SUMO1- and SUMO2/3-modifed proteins that were enriched on nascent DNA molecules when iPOND purifications were analyzed by WB (Figure S1). These results indicate that the replisome vicinity is particularly rich on SUMOylated proteins, further illustrating the role of this modification during DNA replication.

To finalize the analysis, we also generated a table for proteins that were less concentrated on the surroundings of the replisome (EdU) than on overall chromatin (Thy) (Table 2). As mentioned before, an enrichment of histones was evident on Thy fractions, which was also seen for other DNA-binding proteins involved in high-order chromatin structure, such as high-mobility group proteins (HMGA1, HMGA2, and HMGB2). The list also reveals an enrichment of Lamin B1 and BANF1 on mature chromatin, both of which are related to the structure of the nuclear envelope and the Hutchinson-Gilford progeria syndrome (Puente et al., 2011). Finally, iPOND-MS detected a significant and consistent enrichment of ubiquitin (UQ) peptides on all (six out of six, a 4-fold enrichment on average) Thy samples, which was also noticeable by WB (Figure S1). This enrichment of UQ conjugates on mature chromatin samples is in sharp contrast to the enrichment of SUMO on nascent DNA molecules. In some cases, UQylation and SUMOylation are known to occur at the same residue (reviewed in Bergink and Jentsch, 2009). This is best known in the case of PCNA, where SUMO and UQ modifications regulate the loading of alternative polymerases to the replication fork (Hoege et al., 2002). Yet, new examples are also emerging where SUMOylation on one residue could promote the nuclear function of a protein, which would then be counteracted by UQylation on the same residues (Anderson et al., 2012). On the basis of the generalized SUMOylation and concomitant depletion of UQylated proteins we detected on nascent DNA molecules, we propose that this switch from SUMO to UQ could be a general strategy that favors the stability and/or function of proteins residing in the surroundings of the replisome.

Validation of Newly Identified Factors Enriched on Nascent DNA Molecules

To validate the strength of our data set, we tested the enrichment of some of these factors by WB in two new iPOND experiments that were used for validation. In this manner, we were able to confirm an enrichment of UHRF1, ZNF24, and GTF2I on nascent DNA molecules as well as the presence of another known replication factor (RFC3) (Figure S2A). We should note that these proteins were not the only ones tested but, rather, those for which antibodies worked. In all cases tested, WB findings were equivalent to those observed by MS. Moreover, in the case of ZNF24 and with the use of an EGFP fusion protein, we were also able to see its localization to replication factories on the basis of its colocalization with PCNA (Figure S2B).

To provide a more comprehensive validation of the potential role of the identified factors in DNA replication, we selected 19 genes from the list of those that showed enrichment at nascent

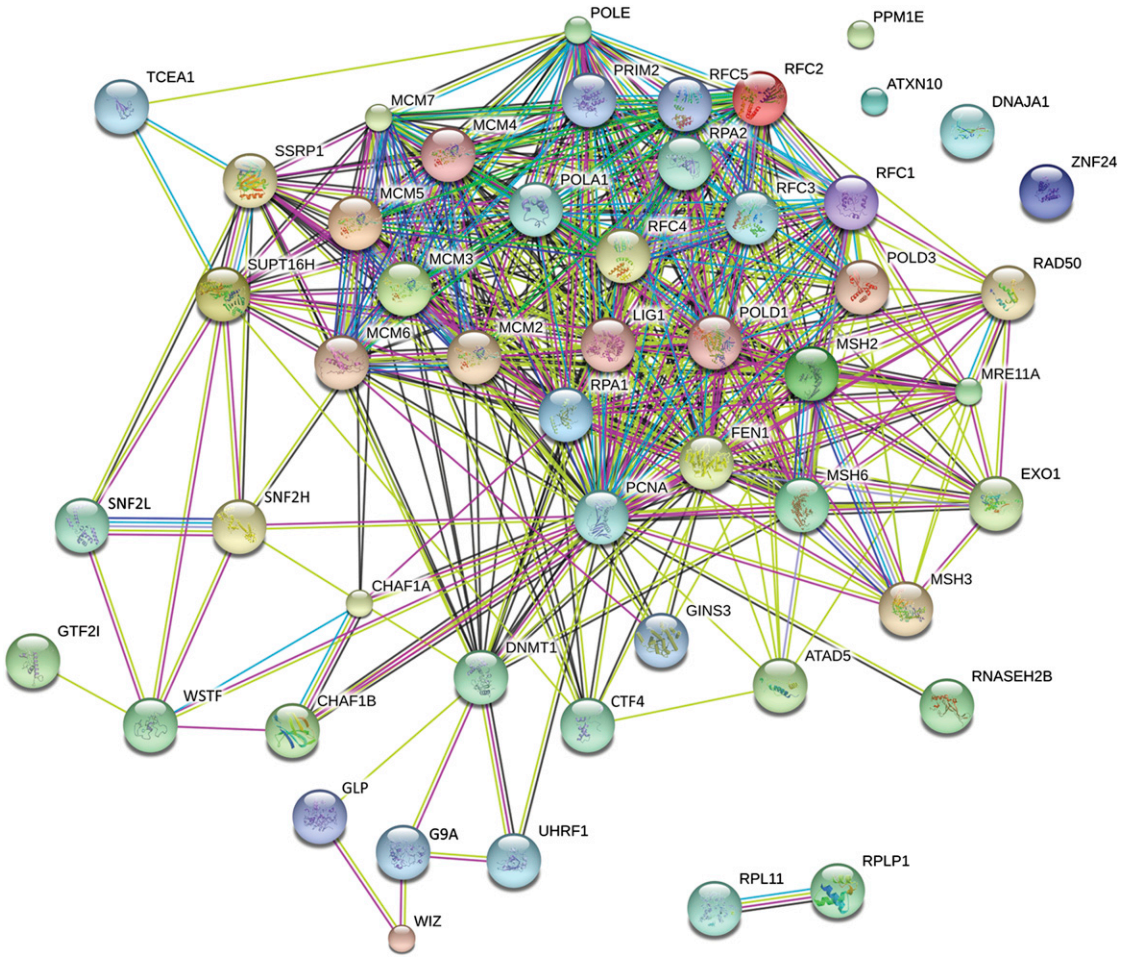

Figure 3. An Interaction Network for Proteins Enriched in Nascent DNA

The image illustrates a network analysis of proteins enriched on nascent DNA molecules (Table1) that was created with STRING. Note that several of the nodes coincide with the functional categories defined in Table 1. The different colors of the connecting lines represent the types of evidence supporting each association: neighborhood (green), gene fusion (red), co-occurrence (blue), coexpression (brown), experiments (pink), databases (cyan), text-mining (yellow), and homology (violet). More details can be found in Results and at http://string.embl.de/.

DNA molecules for additional analyses. The selection concentrated on newly identified factors (see Discussion) but also included known replication factors (PCNA, POLD2, and PRIM2) as controls. For each gene, two siRNAs were used to evaluate the impact of depleting the protein on DNA replication (as compared to the effect of two independent control sequences), which was evaluated by analyzing EdU incorporation through high-throughput microscopy (Figure 4). Depletion of 16 out of the 19 factors (including PCNA, POLD2, and PRIM2) led to a significant reduction in EdU incorporation rates with at least one of the siRNAs. Notably, an increase in EdU incorporation rates was also observed for some of the factors, most obviously for MSH6. Nevertheless, this most likely reflects the activity of MMR on the elimination of dU residues from DNA during S phase (Rada et al., 2004) and not a real increase in DNA replication rates.

Finally, given that EdU incorporation rates could also reflect changes in cell-cycle distribution, we selected two of the newly identified factors (WIZ and ZNF24) and measured the impact of their depletion on replication fork speed through combing analyses of individual DNA molecules (Figure S3). The selection of these two factors was based on previous knowledge, which suggested that these two proteins might be involved in DNA replication (see Discussion). In fact, the depletion of either WIZ or ZNF24 led to a significant downregulation of fork speed. Altogether, the validation experiments further reinforced the strength of the data set supplied in this resource and provided evidence for the role of additional factors involved in DNA replication, most definitively in the case of ZNF24.

DISCUSSION

Identification of Known Replication-Associated Factors by iPOND-MS

The iPOND-MS pipeline used in this study allowed us to provide the most comprehensive proteomic analysis of the human

Table 2. List of Proteins Enriched on the Thy Chase Samples by iPOND-MS

Gene Name	Alias	Enrichment (log2)	No. of Reps
Histone H1.4	**HIST1H1E**	-9.07	5 (5)
Core histone macro-H2A.1	**macroH2A**	-8.74	6 (6)
Histone H2A.Z	**H2A.Z**	-8.17	6 (6)
Histone H1.0	**H1.0**	-7.73	6 (6)
High mobility group protein HMG-I/HMG-Y	**HMGA1**	-8.14	5 (5)
Heterochromatin protein 1-binding protein 3	**HP1BP3**	-8.00	5 (5)
High mobility group protein B2	**HMGB2**	-6.48	4 (5)
High mobility group protein HMGI-C	**HMGA2**	-5.32	4 (5)
Barrier-to-autointegration factor	**BANF1**	-6.81	6 (6)
Lamin-B1	**LMNB1**	-4.02	5 (6)
60S ribosomal protein L17	**RPL17**	-6.82	5 (5)
Ribosomal protein L15	**RPL15**	-6.66	5 (5)
60S ribosomal protein L29	**RPL29**	-6.63	6 (6)
60S ribosomal protein L13	**RPL13**	-6.25	5 (6)
60S ribosomal protein L30	**RPL30**	-6.08	4 (4)
60S ribosomal protein L18	**RPL18**	-6.00	4 (5)
Dystrophin	**DMD**	-11.46	4 (4)
Zinc finger protein 22	**ZNF22**	-7.39	4 (5)
Keratinocyte proline-rich protein	**KPRP**	-7.18	4 (4)
Nuclear ubiquitous casein and cyclin-dependent kinase substrate 1	**NUCKS1**	-6.57	6 (6)
Hepatoma-derived growth factor-related protein 2	**HDGFRP2**	-6.15	5 (5)
Mediator of DNA damage checkpoint protein 1	**MDC1**	-6.11	4 (4)
U2 small nuclear ribonucleoprotein A	**SNRPA1**	-5.73	4 (4)
Serine--tRNA ligase, cytoplasmic	**SARS**	-5.51	4 (4)
Lymphoid-specific helicase	**HELLS**	-4.93	5 (6)
Eukaryotic translation elongation factor 1 epsilon-1	**EEF1E1**	-4.70	4 (4)
Centromere protein V	**CENPV**	-4.53	4 (5)
Nucleoplasmin-3	**NPM3**	-4.50	4 (5)

The cutoff was set in those proteins that were enriched more than 4-fold on the Thy sample (versus EdU) in at least four out of five experiments in which they were detected. Numbers indicate the number of experiments in which the protein was enriched above the established cut-off. Bracketed numbers indicate the number of experiments in which the protein was detected by MS.

replisome and replisome-associated factors reported to date, and we identified the majority of known activities that are needed for DNA replication. PCNA was the protein that showed the highest enrichment on EdU/Thy ratios, followed by MMR proteins MSH2, MSH3, and MSH6 and all members of the clamp loader complex RFC (RFC1–RFC5). Both members of the chromatin assembly factor 1 (CAF1) (CHAF1A and CHAF1B), which deposits nucleosomes on newly replicated chromatin (Alabert and Groth, 2012), followed after that. A recent report also identified a direct interaction between MMR proteins and CAF1 (Schöpf et al., 2012), which could further facilitate the enrichment of CAF1 at nascent DNA molecules.

Substantial enrichment of the ssDNA-binding complex RPA (RPA1 and RPA2) was also found on the EdU fraction, confirming that our purification pipeline was also pulling down regions of ssDNA on EdU samples. The list was followed by all the necessary DNA polymerases that are associated with unperturbed DNA replication (Hübscher, 2009): the catalytic subunit and primase from the polymerase alpha complex (POLA1/PRIM2), which initiates DNA synthesis at replication origins and from Okazaki fragments; and polymerases delta (POLD1 and POLD3) and epsilon (POLE) that, at least in yeast, are in charge of replicating lagging and leading strands, respectively. The next protein on the list was CTF4, a cohesion-related factor in yeast that was identified two decades ago as an interactor of polymerase alpha (Miles and Formosa, 1992) and has again been found in more recent proteomic studies in yeast as an essential component that couples helicases with DNA polymerase alpha (Gambus et al., 2006; 2009). Next, we included a group of activities involved in the maturation of Okazaki fragments such as DNA ligase (LIG1), exonuclease (EXO1), ribonuclease (RNASEH2B), and flap endonuclease (FEN1). Members of the MCM helicases and its associated complex go ichi ni san (GINS) were found next, followed by the two subunits of the FACT histone chaperone complex (SUPT16H and SSRP1). The FACT complex has also been previously observed in association with the replisome and MCM proteins and is thought to provide properly folded and assembled nucleosomes to newly synthesized chromatin (Gambus et al., 2006; Tan et al., 2006).

Of the 32 proteins mentioned so far, which were ordered on the basis of their enrichment on our iPOND-MS samples, all

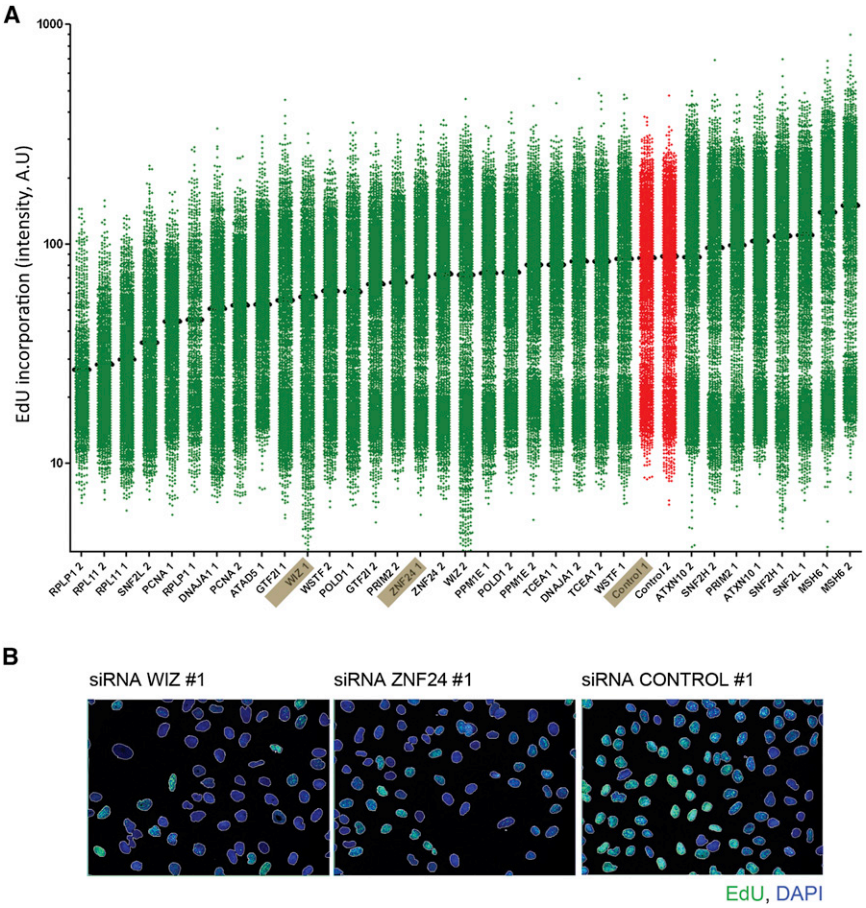

Figure 4. Screening for Factors that Decrease Overall DNA Replication Rates

(A) The data illustrate the evaluation of EdU incorporation rates in U2OS cells that were transfected with the indicated siRNA sequences and evaluated 36 hr after transfection by high-throughput microscopy. Each dot represents the mean EdU signal per nucleus for each condition after a 1 hr pulse with EdU (10 μM). Two independent siRNA sequences were used per gene (green), including two different controls (highlighted in red). Three samples (control, WIZ, and ZNF24) for which images are shown below are indicated by a gray shadow over the gene name.

(B) Representative examples of the images obtained in (A) for the three siRNA sequences indicated above. EdU (green) and DAPI (blue) channels are shown. Segmentation of the nuclei was done with the use of a DAPI signal (nuclei are surrounded with a white line).

have a remarkably well-established connection with replication. Notably, the absence of a known replication protein from this list does not indicate an absence of enrichment around replisomes but, rather, reflects that the protein was not detected by MS, or at least not enough times to pass our stringency filters and make it to the final list. Nevertheless, even in those cases in which known replication-associated proteins were only detected once, they invariably showed a significant enrichment at nascent DNA molecules (the full data set is available in Table S1). From here on, we comment on the remaining list of proteins that passed our filters for enrichment on nascent DNA molecules and that have already been linked to DNA replication.

Restoring DNA and Histone Methylation on Newly Replicated DNA

The first group includes a set of proteins that are involved in DNA (DNMT1) or histone (G9A and the G9A-associated protein GLP) methylation, all of which have been found to interact at replication foci (Estève et al., 2006). As part of this group, we included WIZ, which was shown in a complex with the G9A-GLP histone methyltransferase (Ueda et al., 2006), and UHRF1, which is a multidomain protein that coordinates all the activities from this group. UHRF1 binds hemimethylated DNA, brings DNMT1 to replicated regions, and interacts with G9A-GLP (Bostick et al., 2007; Sharif et al., 2007; Kim et al., 2009), providing a scaffold that can recognize chromatin methylation and allow its maintenance. As a group, this set of proteins would be in charge of restoring DNA and histone methylation marks on newly replicated chromatin. This group of proteins is, in fact, recognized as a node in STRING analyses (Figure 3). Our validation data support a role for UHRF1 and, most clearly for, WIZ in DNA replication. Moreover, WIZ overexpression promotes resistance to drugs inhibiting DNA replication (Levenson et al., 1999). How WIZ promotes DNA replication, or if this activity is linked to the G9A complex, remains to be clarified.

The MRN Complex during S Phase

Besides MMR proteins, which correct mismatches introduced by DNA polymerases, the only DNA repair factors that showed a consistent and significant enrichment in nascent DNA molecules were MRE11 and RAD50, members of the MRN (MRE11-RAD50-NBS1) complex. The third member of the complex, NBS1, was detected only once in our iPOND-MS but also showed a clear enrichment on the EdU fraction. Although the complex is mostly known for its role in DNA repair, early studies already noted a preferential location of MRN proteins at replication factories (Maser et al., 2001; Mirzoeva and Petrini, 2003) and that the complex was necessary to prevent genomic breakage during replication (Costanzo et al., 2001). In addition, several recent studies have revisited an active role for MRN, particularly for the nuclease activity of MRE11, on the nucleolitic degradation of stalled replication forks (reviewed in Costanzo, 2011). The fact that MRN is the only DNA double-strand-break-repair-associated complex that we find in our list further underscores the key role of this complex during normal replication.

An Association with the Williams-Beuren Syndrome

The Williams-Beuren syndrome (WBS) is a human disease characterized by mental retardation and cardiac malfunction and is linked to the deletion of around 20 genes at chromosome 7q11.23 (OMIM 194050). The first gene from this region that was identified as related with WBS was the Williams syndrome transcription factor (WSTF) (Peoples et al., 1998), which is clearly enriched in our EdU samples. Recent studies have identified that WSTF forms a complex with the ISWI-type ATPase SNF2H, which is targeted to replisomes through an interaction with PCNA (Poot et al., 2004). Besides WSTF, SNF2L and SNF2H were clearly enriched on our iPOND-MS, although SNF2H was just below our stringency filter (4-fold mean enrichment). Although no physical interaction with WSTF or SNF2 is known, our analysis also found the general transcription factor II-1 (GTF2I) among the enriched factors, its gene being located at the locus that is deleted on the WBS. In fact, GTF2I enrichment on nascent DNA molecules was verified by WB, (Figure S2) and GTF2I depletion decreased EdU incorporation rates (Figure 4). STRING analyses also place GTF2I, WSTF, SNF2H, and SNF2L within a functional node (see Figure 3). Finally, it is worth mentioning that RFC2 is also one of the 20 genes that are deleted on the WBS locus. Given the small size of the locus and the number of proteins associated to WBS that are present in our list, we believe that these findings support a possible connection between WBS and DNA replication.

Additional Proteins Enriched at Nascent DNA Molecules

Nine additional polypeptides with no obvious connection to replication were also identified as enriched in nascent DNA: PPM1E, ZNF24, ATAD5, RPLP1, TUBB4, RPL11, DNAJA1, ATXN10, and TCEA1. From this list, the only hint of a direct connection with replication is with ATAD5, also known as ELG1, which regulates the lifespan of DNA replication factories by limiting the levels of chromatin-bound PCNA through its deubiquitinylation (Lee et al., 2010; 2013). Interestingly, a recent study using Dm-ChP also found an enrichment of ribosomal proteins (such as RPLP1 and RPL11) on pulled-down EdU fractions (Kliszczak et al., 2011). Moreover, a connection between the DNA replication machinery and ribosomal biogenesis was first detected in proteomic studies in yeast (Du and Stillman, 2002), and RPLP1 and RPL11 depletion led to the highest decrease in EdU incorporation in our validation analyses (Figure 4). Still, because of the potential pleotropic effects of disturbing ribosome stability, the functional meaning of these interactions remains unknown.

ZNF24 as a Newly Identified DNA Replication Factor

Of all the factors identified in this study, most data support a role of ZNF24 in DNA replication. Moreover, a review of the existing literature would be consistent with ZNF24 playing an important role in DNA replication. First, its expression is most abundant on proliferating areas during embryonic development (Khalfallah et al., 2008). Second, knockdown of ZNF24 limits the growth of neural stem cells (Khalfallah et al., 2009) or hepatocarcinoma cell lines (Liu et al., 2012), and full deletion is early embryonic lethal in the mouse (Li et al., 2006). Third, ZNF24 is SUMOylated (Gocke et al., 2005) and phosphorylated by ATM and ATR kinases (Matsuoka et al., 2007), both modifications being abundant at replication forks. In this study, we confirmed a substantial enrichment of ZNF24 at nascent DNA molecules and showed that it colocalizes with PCNA at replication factories. In addition, ZNF24 depletion decreased overall EdU incorporation rates in cell culture and replication fork speed when measured on single DNA molecules. In summary, and in the context of the previously available literature, the data provided in this work strongly indicate that ZNF24 is a newly identified player in the control of DNA replication.

Conclusion

Here, we provide a proteomic characterization of the human replisome vicinity derived from iPOND purification of nascent DNA molecules. Our modifications on the protocol and the high stringency for the selection of enriched factors facilitated a restrictive identification of factors that are enriched in close proximity to the replication forks. Our table provides the most comprehensive repository of replisome and replisome-associated factors isolated from the same experiment published to date, identifying a large fraction of the known replication factors as well as several other proteins with distant or no previous association with DNA replication. As a proof of concept of the usefulness of this resource, we have provided data supporting a link between WBS and DNA replication, identified ZNF24 as a DNA replication factor, and uncovered an opposite accumulation of UQ and SUMO modified proteins in the replisome vicinity. Altogether, we believe that our results validate the iPOND-MS strategy as a solid proteomic approach for the identification of replication-associated factors and their posttranslational modifications and provide a valuable resource that should be of help for investigators working on DNA replication, recombination, and repair.

EXPERIMENTAL PROCEDURES

Cell Culture

All the experiments were performed in human *HEK293T* cells. HEK cells were grown in Dulbecco's minimum essential media (DMEM, Invitrogen) supplemented with 10% fetal bovine serum (Sigma-Aldrich) and antibiotics.

iPOND

We followed the iPOND protocol described in Sirbu et al., 2012, with a few modifications. In brief, 1.5×10^8 293T cells (per condition) were plated in six 15 cm plates the day before the experiment. On the following day, 10 μM EdU (Invitrogen) was added to the medium for 10 min. For the chase condition, the EdU treatment was followed by three thorough washes in PBS and a subsequent incubation in medium to which 10 μM Thymidine (Sigma-Aldrich) was added for the indicated times. Afterward, cells were fixed with 1% formaldehyde for 15 min, which also generated DNA-protein and protein-protein crosslinks. Then, cells were scraped from the plate, permeabilized (0.25% Triton X-100 in PBS, 30 min at room temperature), and subjected to the Click-iT reaction with the use of Biotin Azide (Invitrogen). Cell lysis (1% SDS in 50 mM Tris [pH 8]) and sonication followed. We used a different sonication schedule and a higher dilution of cells in the lysis buffer than the one described in Sirbu et al., 2012, which facilitated the purification of smaller chromatin fragments. For each condition, 35×10^8 cells were resuspended in 7 ml of lysis buffer and sonicated with a Bioruptor (Diagenode) for 20 min in 30 s on/off cycles at high intensity. Finally, EdU-biotin-labeled DNA was pulled down with the use of streptavidin-agarose beads (Novagen). We added 250 μl of beads to each sample and incubated them at 4°C for 20 hr. Then, the beads were washed twice with lysis buffer and NaCl 1M and eluted in 100 μl

of 25× NuPAGE LDS Sample Buffer (Invitrogen) containing 10% β-mercaptoethanol (25 min at 95°C). Protease inhibitor cocktail tablets (Roche) and phenylmethanesulfonylfluoride (Sigma-Aldrich) were added to all buffers.

Immunoblotting

Samples were resolved by SDS-PAGE and analyzed by standard WB techniques. Antibodies against PCNA (Santa-Cruz Biotechnology), β-actin, and POLD2 (Sigma-Aldrich), MSH2 (Calbiochem), UHRF1, RF3, and RFC4 (GeneTex), ZNF24 and GTF2I (Novus Biologicals), SUMO1 and Histone H4 (Abcam), and SUMO2/3 (MBL International) were used. Protein blot analyses were performed on the LI-COR platform (LI-COR Biosciences).

Protein Digestion

Eluates were digested with the use of the filter aided sample preparation (FASP) method (Wiśniewski et al., 2009) with some modifications. In brief, each sample was dissolved in 8 M urea in 0.1 M Tris/HCl (pH 8.5) (UA) and loaded onto centrifugal devices Nanosep 30K Omega (Pall). The elution buffer was completely replaced by washing three to four times with UA. Proteins were then alkylated using 50 mM iodoacetamide for 20 min in the dark and the excess of alkylation reagents was washed out with UA. Proteins were digested overnight with the use of endoproteinase Lys-C (Wako Pure Chemicals Industries) and diluted in 50 mM ammonium bicarbonate. Finally, trypsin (Promega) was added, and samples were subjected to a second digestion for 6 hr. Resulting peptides were cleaned up by homemade columns on the basis of Stage Tips with C18 Empore Disks (3 M) (Rappsilber et al., 2003) filled with R3 resin (Applied Biosystems). Eluates were evaporated to dryness and dissolved in 0.1% formic acid (FA).

NanoLC Tandem Mass Spectrometry

Peptides were separated by the online reversed-phase NanoLC Ultra 1D Plus system (Eksigent Technologies) and analyzed with the use of a LTQ Orbitrap Velos mass spectrometrer (Thermo Scientific) equipped with a nanoelectrospray ion source (Proxeon Biosystems). Solvent A was 0.1% FA, and solvent B was acetonitrile in 0.1% FA. Samples (10 μl injections) were loaded onto a reversed-phase ReproSil Pur C18-Aq 5 μm 0.3 × 10 mm trapping column (SGE Analytical Science) and washed for 15 min at 2.5 μL/min with solvent A. The peptides were eluted onto an analytical column consisting of ReproSil Pur C18-AQ 3 μm 200 × 0.075 mm (Dr. Maisch). The following gradient was used: 0–2 min 2% B, 2–80 min 2%–24% B, 80–122 min 24%–40% B, 122–123 min 40%–98% B, 123–130 min 98% B, and 131–145 min 2% B. The flow rate was 300 nL/min. The column was operated at a constant temperature of 30°C.

The LTQ Orbitrap Velos was operated in positive ionization mode. The spray voltage was set to 1.5 kV, and the temperature of the heated capillary was set to 275°C. The MS survey scan was performed in the FT analyzer scanning a window between 250 and 1750 *m/z*. The resolution was set to 60,000 FWHM at *m/z* 400. The *m/z* values triggering tandem mass spectrometry (MS/MS) with a repeat count of one were put on an exclusion list for 40 s. The minimum MS signal for triggering MS/MS was set to 1,000 counts. In all cases, one microscan was recorded. The lock mass option was enabled for both MS and MS/MS mode and the polydimethylcyclosiloxane ions (PDMS, protonated $(Si(CH_3)_2O)_6$; *m/z* 445.120025) were used for internal recalibration of the mass spectra (Olsen et al., 2005). For the collisionally induced dissociation (CID/CAD), up to 20 of the most abundant isotope patterns with a charge ≥ 2 from the survey scan were selected with an isolation window of 2 *m/z* and fragmented in the linear ion trap. Normalized collision energy was set to 35%, the q value was set to 0.25, and the activation time was set to 10 ms. The maximum ion injection times for the survey scan and the MS/MS scans were 500 and 150 ms, respectively, and the ion target values were set to 1×10^6 and 5,000, respectively, for each scan mode.

Data Analysis

Raw data were processed by MaxQuant (Cox and Mann, 2008) version 1.3.0.3. Maximum false discovery rates were set to 0.01 for both the protein and peptide. Peak lists were searched against UniProt human database, and Andromeda (Cox et al., 2011) was used as a search engine. N-terminal acetylation and methionine oxidation were set as variable modifications, and the carbamidomethylation of cysteine residues was set as fixed modification. Analysis was limited to peptides of seven or more amino acids and maximum two missed cleavages. In the case that identified peptides were shared by two or more proteins (homologs or isoforms), they were reported by MaxQuant as one protein group. The analysis of functional groups and potential interactions for the list of enriched proteins was done with the IPA (Ingenuity Systems) and STRING (von Mering et al., 2003) (http://string-db.org) softwares, respectively.

High-Throughput Microscopy of EdU Incorporation

U2OS cells were transfected with two independent small interfering RNAs (siRNAs) per gene (Silencer Select, Life Technologies; sequences are available upon request) at 50 nM using Lipofectamine RNAiMAX (Life Technologies). On the following day, cells were plated on μCLEAR bottom 96-well plates (Greiner Bio-One), and EdU incorporation analyses were performed 36 hr after transfection. In brief, 10 μM EdU was added to the culture media for 1 hr. Cells were washed with PBS, fixed with 2% paraformaldehyde for 10 min, and permeabilized with 0.5% Triton for 15 min and then EdU was detected performing Click-iT with Alexa Flour 488 Azide (Life Technologies). Images were automatically acquired from each well by an Opera High-Content Screening System (PerkinElmer) with a 20× magnification lens and nonsaturating exposure times. Images were segmented with a DAPI signal to generate masks matching cell nuclei from which the mean EdU signal was calculated. Data were represented with the use of the Prism software (GraphPad Software).

DNA Combing

U2OS cells were transfected with the indicated siRNA sequences. Cells were pulse-labeled consecutively with 50 μM CldU (20 min) and 250 μM IdU (20 min) 36 hr after transfection. DNA fibers were prepared and stained as described previously (Terret et al., 2009). Fork progression rate was measured from >200 tracks per sample, and statistical analysis was conducted with the use of a Mann-Whitney rank sum test.

SUPPLEMENTAL INFORMATION

Supplemental Information includes three figures and one table and can be found with this article online at http://dx.doi.org/10.1016/j.celrep.2013.03.009.

LICENSING INFORMATION

ACKNOWLEDGMENTS

A.J.L. is the recipient of a postdoctoral fellowship from the Spanish Association Against Cancer (AECC). M.N. and S.R. are funded by Ph.D. fellowships from the La Caixa Foundation. Work in O.F.'s laboratory is supported by grants from the Spanish Ministry of Economy (SAF2011-23753 and CSD2007-00017), the Association for International Cancer Research (12-0229), the Howard Hughes Medical Institute, and the European Research Council (ERC-210520). Work in J.M.'s laboratory is supported by grants from the Spanish Ministry of Economy (BFU2010-21467 and CSD2007-00015).

Received: November 28, 2012
Revised: February 13, 2013
Accepted: March 8, 2013
Published: March 28, 2013

REFERENCES

Alabert, C., and Groth, A. (2012). Chromatin replication and epigenome maintenance. Nat. Rev. Mol. Cell Biol. *13*, 153–167.

Anderson, D.D., Eom, J.Y., and Stover, P.J. (2012). Competition between sumoylation and ubiquitination of serine hydroxymethyltransferase 1

determines its nuclear localization and its accumulation in the nucleus. J. Biol. Chem. *287*, 4790–4799.

Aparicio, T., Megías, D., and Méndez, J. (2012). Visualization of the MCM DNA helicase at replication factories before the onset of DNA synthesis. Chromosoma *121*, 499–507.

Bergink, S., and Jentsch, S. (2009). Principles of ubiquitin and SUMO modifications in DNA repair. Nature *458*, 461–467.

Bostick, M., Kim, J.K., Estève, P.-O., Clark, A., Pradhan, S., and Jacobsen, S.E. (2007). UHRF1 plays a role in maintaining DNA methylation in mammalian cells. Science *317*, 1760–1764.

Cappella, P., Gasparri, F., Pulici, M., and Moll, J. (2008). A novel method based on click chemistry, which overcomes limitations of cell cycle analysis by classical determination of BrdU incorporation, allowing multiplex antibody staining. Cytometry A *73*, 626–636.

Cimprich, K.A., and Cortez, D. (2008). ATR: an essential regulator of genome integrity. Nat. Rev. Mol. Cell Biol. *9*, 616–627.

Clark, A.B., Valle, F., Drotschmann, K., Gary, R.K., and Kunkel, T.A. (2000). Functional interaction of proliferating cell nuclear antigen with MSH2-MSH6 and MSH2-MSH3 complexes. J. Biol. Chem. *275*, 36498–36501.

Cook, P.R. (1999). The organization of replication and transcription. Science *284*, 1790–1795.

Costanzi, C., and Pehrson, J.R. (1998). Histone macroH2A1 is concentrated in the inactive X chromosome of female mammals. Nature *393*, 599–601.

Costanzo, V. (2011). Brca2, Rad51 and Mre11: performing balancing acts on replication forks. DNA Repair (Amst.) *10*, 1060–1065.

Costanzo, V., Robertson, K., Bibikova, M., Kim, E., Grieco, D., Gottesman, M., Carroll, D., and Gautier, J. (2001). Mre11 protein complex prevents double-strand break accumulation during chromosomal DNA replication. Mol. Cell *8*, 137–147.

Cox, J., and Mann, M. (2008). MaxQuant enables high peptide identification rates, individualized p.p.b.-range mass accuracies and proteome-wide protein quantification. Nat. Biotechnol. *26*, 1367–1372.

Cox, J., Neuhauser, N., Michalski, A., Scheltema, R.A., Olsen, J.V., and Mann, M. (2011). Andromeda: a peptide search engine integrated into the MaxQuant environment. J. Proteome Res. *10*, 1794–1805.

Du, Y.-C.N., and Stillman, B. (2002). Yph1p, an ORC-interacting protein: potential links between cell proliferation control, DNA replication, and ribosome biogenesis. Cell *109*, 835–848.

Estève, P.-O., Chin, H.G., Smallwood, A., Feehery, G.R., Gangisetty, O., Karpf, A.R., Carey, M.F., and Pradhan, S. (2006). Direct interaction between DNMT1 and G9a coordinates DNA and histone methylation during replication. Genes Dev. *20*, 3089–3103.

Gambus, A., Jones, R.C., Sanchez-Diaz, A., Kanemaki, M., van Deursen, F., Edmondson, R.D., and Labib, K. (2006). GINS maintains association of Cdc45 with MCM in replisome progression complexes at eukaryotic DNA replication forks. Nat. Cell Biol. *8*, 358–366.

Gambus, A., van Deursen, F., Polychronopoulos, D., Foltman, M., Jones, R.C., Edmondson, R.D., Calzada, A., and Labib, K. (2009). A key role for Ctf4 in coupling the MCM2-7 helicase to DNA polymerase alpha within the eukaryotic replisome. EMBO J. *28*, 2992–3004.

Gocke, C.B., Yu, H., and Kang, J. (2005). Systematic identification and analysis of mammalian small ubiquitin-like modifier substrates. J. Biol. Chem. *280*, 5004–5012.

Hoege, C., Pfander, B., Moldovan, G.L., Pyrowolakis, G., and Jentsch, S. (2002). RAD6-dependent DNA repair is linked to modification of PCNA by ubiquitin and SUMO. Nature *419*, 135–141.

Hübscher, U. (2009). DNA replication fork proteins. Methods Mol. Biol. *521*, 19–33.

Jiricny, J. (2006). The multifaceted mismatch-repair system. Nat. Rev. Mol. Cell Biol. *7*, 335–346.

Khalfallah, O., Faucon-Biguet, N., Nardelli, J., Meloni, R., and Mallet, J. (2008). Expression of the transcription factor Zfp191 during embryonic development in the mouse. Gene Expr. Patterns *8*, 148–154.

Khalfallah, O., Ravassard, P., Lagache, C.S., Fligny, C., Serre, A., Bayard, E., Faucon-Biguet, N., Mallet, J., Meloni, R., and Nardelli, J. (2009). Zinc finger protein 191 (ZNF191/Zfp191) is necessary to maintain neural cells as cycling progenitors. Stem Cells *27*, 1643–1653.

Kim, J.K., Estève, P.-O., Jacobsen, S.E., and Pradhan, S. (2009). UHRF1 binds G9a and participates in p21 transcriptional regulation in mammalian cells. Nucleic Acids Res. *37*, 493–505.

Kliszczak, A.E., Rainey, M.D., Harhen, B., Boisvert, F.M., and Santocanale, C. (2011). DNA mediated chromatin pull-down for the study of chromatin replication. Sci. Rep. *1*.

Kolb, H.C., Finn, M.G., and Sharpless, K.B. (2001). Click Chemistry: Diverse Chemical Function from a Few Good Reactions. Angew. Chem. Int. Ed. Engl. *40*, 2004–2021.

Laskey, R.A., and Madine, M.A. (2003). A rotary pumping model for helicase function of MCM proteins at a distance from replication forks. EMBO Rep. *4*, 26–30.

Lee, K.-Y., Yang, K., Cohn, M.A., Sikdar, N., D'Andrea, A.D., and Myung, K. (2010). Human ELG1 regulates the level of ubiquitinated proliferating cell nuclear antigen (PCNA) through Its interactions with PCNA and USP1. J. Biol. Chem. *285*, 10362–10369.

Lee, K.Y., Fu, H., Aladjem, M.I., and Myung, K. (2013). ATAD5 regulates the lifespan of DNA replication factories by modulating PCNA level on the chromatin. J. Cell Biol. *200*, 31–44.

Leonhardt, H., Rahn, H.P., Weinzierl, P., Sporbert, A., Cremer, T., Zink, D., and Cardoso, M.C. (2000). Dynamics of DNA replication factories in living cells. J. Cell Biol. *149*, 271–280.

Levenson, V.V., Lausch, E., Kirschling, D.J., Broude, E.V., Davidovich, I.A., Libants, S., Fedosova, V., and Roninson, I.B. (1999). A combination of genetic suppressor elements produces resistance to drugs inhibiting DNA replication. Somat. Cell Mol. Genet. *25*, 9–26.

Li, J., Chen, X., Yang, H., Wang, S., Guo, B., Yu, L., Wang, Z., and Fu, J. (2006). The zinc finger transcription factor 191 is required for early embryonic development and cell proliferation. Exp. Cell Res. *312*, 3990–3998.

Liu, G., Jiang, S., Wang, C., Jiang, W., Liu, Z., Liu, C., Saiyin, H., Yang, X., Shen, S., Jiang, D., et al. (2012). Zinc finger transcription factor 191, directly binding to β-catenin promoter, promotes cell proliferation of hepatocellular carcinoma. Hepatology *55*, 1830–1839.

López-Contreras, A.J., and Fernandez-Capetillo, O. (2010). The ATR barrier to replication-born DNA damage. DNA Repair (Amst.) *9*, 1249–1255.

Luber, C.A., Cox, J., Lauterbach, H., Fancke, B., Selbach, M., Tschopp, J., Akira, S., Wiegand, M., Hochrein, H., O'Keeffe, M., and Mann, M. (2010). Quantitative proteomics reveals subset-specific viral recognition in dendritic cells. Immunity *32*, 279–289.

Maga, G., Villani, G., Tillement, V., Stucki, M., Locatelli, G.A., Frouin, I., Spadari, S., and Hübscher, U. (2001). Okazaki fragment processing: modulation of the strand displacement activity of DNA polymerase delta by the concerted action of replication protein A, proliferating cell nuclear antigen, and flap endonuclease-1. Proc. Natl. Acad. Sci. USA *98*, 14298–14303.

Maser, R.S., Mirzoeva, O.K., Wells, J., Olivares, H., Williams, B.R., Zinkel, R.A., Farnham, P.J., and Petrini, J.H. (2001). Mre11 complex and DNA replication: linkage to E2F and sites of DNA synthesis. Mol. Cell. Biol. *21*, 6006–6016.

Matsuoka, S., Ballif, B.A., Smogorzewska, A., McDonald, E.R., 3rd, Hurov, K.E., Luo, J., Bakalarski, C.E., Zhao, Z., Solimini, N., Lerenthal, Y., et al. (2007). ATM and ATR substrate analysis reveals extensive protein networks responsive to DNA damage. Science *316*, 1160–1166.

Miles, J., and Formosa, T. (1992). Protein affinity chromatography with purified yeast DNA polymerase alpha detects proteins that bind to DNA polymerase. Proc. Natl. Acad. Sci. USA *89*, 1276–1280.

Mirzoeva, O.K., and Petrini, J.H.J. (2003). DNA replication-dependent nuclear dynamics of the Mre11 complex. Mol. Cancer Res. *1*, 207–218.

Mizuguchi, G., Shen, X., Landry, J., Wu, W.H., Sen, S., and Wu, C. (2004). ATP-driven exchange of histone H2AZ variant catalyzed by SWR1 chromatin remodeling complex. Science *303*, 343–348.

Nekrasov, M., Amrichova, J., Parker, B.J., Soboleva, T.A., Jack, C., Williams, R., Huttley, G.A., and Tremethick, D.J. (2012). Histone H2A.Z inheritance during the cell cycle and its impact on promoter organization and dynamics. Nat. Struct. Mol. Biol. *19*, 1076–1083.

Olsen, J.V., de Godoy, L.M.F., Li, G., Macek, B., Mortensen, P., Pesch, R., Makarov, A., Lange, O., Horning, S., and Mann, M. (2005). Parts per million mass accuracy on an Orbitrap mass spectrometer via lock mass injection into a C-trap. Mol. Cell. Proteomics *4*, 2010–2021.

Peoples, R.J., Cisco, M.J., Kaplan, P., and Francke, U. (1998). Identification of the WBSCR9 gene, encoding a novel transcriptional regulator, in the Williams-Beuren syndrome deletion at 7q11.23. Cytogenet. Cell Genet. *82*, 238–246.

Petermann, E., Orta, M.L., Issaeva, N., Schultz, N., and Helleday, T. (2010). Hydroxyurea-stalled replication forks become progressively inactivated and require two different RAD51-mediated pathways for restart and repair. Mol. Cell *37*, 492–502.

Poot, R.A., Bozhenok, L., van den Berg, D.L.C., Steffensen, S., Ferreira, F., Grimaldi, M., Gilbert, N., Ferreira, J., and Varga-Weisz, P.D. (2004). The Williams syndrome transcription factor interacts with PCNA to target chromatin remodelling by ISWI to replication foci. Nat. Cell Biol. *6*, 1236–1244.

Puente, X.S., Quesada, V., Osorio, F.G., Cabanillas, R., Cadiñanos, J., Fraile, J.M., Ordóñez, G.R., Puente, D.A., Gutiérrez-Fernández, A., Fanjul-Fernández, M., et al. (2011). Exome sequencing and functional analysis identifies BANF1 mutation as the cause of a hereditary progeroid syndrome. Am. J. Hum. Genet. *88*, 650–656.

Rada, C., Di Noia, J.M., and Neuberger, M.S. (2004). Mismatch recognition and uracil excision provide complementary paths to both Ig switching and the A/T-focused phase of somatic mutation. Mol. Cell *16*, 163–171.

Rappsilber, J., Ishihama, Y., and Mann, M. (2003). Stop and go extraction tips for matrix-assisted laser desorption/ionization, nanoelectrospray, and LC/MS sample pretreatment in proteomics. Anal. Chem. *75*, 663–670.

Salic, A., and Mitchison, T.J. (2008). A chemical method for fast and sensitive detection of DNA synthesis in vivo. Proc. Natl. Acad. Sci. USA *105*, 2415–2420.

Schöpf, B., Bregenhorn, S., Quivy, J.-P., Kadyrov, F.A., Almouzni, G., and Jiricny, J. (2012). Interplay between mismatch repair and chromatin assembly. Proc. Natl. Acad. Sci. USA *109*, 1895–1900.

Sharif, J., Muto, M., Takebayashi, S.-I., Suetake, I., Iwamatsu, A., Endo, T.A., Shinga, J., Mizutani-Koseki, Y., Toyoda, T., Okamura, K., et al. (2007). The SRA protein Np95 mediates epigenetic inheritance by recruiting Dnmt1 to methylated DNA. Nature *450*, 908–912.

Sirbu, B.M., Couch, F.B., Feigerle, J.T., Bhaskara, S., Hiebert, S.W., and Cortez, D. (2011). Analysis of protein dynamics at active, stalled, and collapsed replication forks. Genes Dev. *25*, 1320–1327.

Sirbu, B.M., Couch, F.B., and Cortez, D. (2012). Monitoring the spatiotemporal dynamics of proteins at replication forks and in assembled chromatin using isolation of proteins on nascent DNA. Nat. Protoc. *7*, 594–605.

Tan, B.C.-M., Chien, C.-T., Hirose, S., and Lee, S.-C. (2006). Functional cooperation between FACT and MCM helicase facilitates initiation of chromatin DNA replication. EMBO J. *25*, 3975–3985.

Terret, M.-E., Sherwood, R., Rahman, S., Qin, J., and Jallepalli, P.V. (2009). Cohesin acetylation speeds the replication fork. Nature *462*, 231–234.

Ueda, J., Tachibana, M., Ikura, T., and Shinkai, Y. (2006). Zinc finger protein Wiz links G9a/GLP histone methyltransferases to the co-repressor molecule CtBP. J. Biol. Chem. *281*, 20120–20128.

von Mering, C., Huynen, M., Jaeggi, D., Schmidt, S., Bork, P., and Snel, B. (2003). STRING: a database of predicted functional associations between proteins. Nucleic Acids Res. *31*, 258–261.

Wiśniewski, J.R., Zougman, A., Nagaraj, N., and Mann, M. (2009). Universal sample preparation method for proteome analysis. Nat. Methods *6*, 359–362.

Worcel, A., Han, S., and Wong, M.L. (1978). Assembly of newly replicated chromatin. Cell *15*, 969–977.

Zhang, R., Poustovoitov, M.V., Ye, X., Santos, H.A., Chen, W., Daganzo, S.M., Erzberger, J.P., Serebriiskii, I.G., Canutescu, A.A., Dunbrack, R.L., et al. (2005). Formation of MacroH2A-containing senescence-associated heterochromatin foci and senescence driven by ASF1a and HIRA. Dev. Cell *8*, 19–30.